Supplementary information

Description of the semi-automated method to generate CLIO bathymetries

This method remplaces the tedious manual changes that have been done on the CLIO grid in the past, in order to be able to generate a CLIO bathymetry quickly from any topography file - a technical development which fastens the start of new PMIP phases and enables the run of transient simulations with an interactive bathymetry. It has been used here to (re)generate a pre-industrial bathymetry (using the high resolution etopo1 topography), a PMIP2 bathymetry (using the ICE-5G reconstruction), and two PMIP4 bathymetries (using either the GLAC-1D or the ICE-6G-C reconstruction).

This development has been done in several pre-processing steps :

— Anomalies are computed using the PMIP2/PMIP4 topographies and then regridded on the etopo1 grid :

LGM topography = PI (etopo1) + LGM Peltier (ICE-6G-C, 21kyr) - PI Peltier (ICE-6G-C, 0kyr)

— A connectivity program (Paillard, pers. com.) writes the mean bathymetry and hypsometry into a text file, either on the rotated or regular CLIO grid. It also produces the connections between ocean basins thanks to the computation of subgrid sills.

— In a second program, the two grids are first put together.

— Then, the mask is generated using the hypsometry, a chosen sea-level (-0.5 m for the PI, -133.9 m for the LGM, according to Lambeck et al. [2014]), and a chosen threshold (% of surface of a grid cell above which the cell is defined as ocean - here 40 %). Small isolated seas are closed. The mask of a few ocean grid cells is manually forced at the PI so that all the critical traits stay open. These manual points have to be redefined at the LGM. Indeed, while some stay the same (Gibraltar), others are not necessary anymore (Hudson Bay and Japan Sea outlets) and a few new critical points appear (Fram Strait, Golf of Mexico outlet). We take particular care of this step, using the connections computed earlier and our knowledge of the LGM ocean.

— The bathymetry is converted into the irregular vertical levels of the CLIO model. The old vertical level is forced for a few problematic grid cells in order to get realistic salinity values in the Mediterranean Sea and Hudson Bay. The vertical level 1 is avoided (either forced to 0 or 2), because the model cannot deal with these very shallow grid cells. As the model also cannot deal with isolated oceanic grid cells for which the last vertical level is isolated (e.g. deep grid cells with shallower neighbours), a process similar to a smoothing filter is applied.

— Finally, this program writes a text file containing the bathymetry with the land-sea mask (0 in every land grid cells).

— Two additional pre-processing steps are required to generate the necessary input files (one containing the fraction of ocean seen by the T21 grid cells, another containing the interpolation points between the CLIO and the T21 grids).

— In order to be able to quickly equilibrate the model when running a simulation with a different bathymetry than its restart, the initialization code of iLOVECLIM has been modified to generate realistic values of the tracers content of new oceanic grid cells. To achieve this, the initialization of all the restart variables in new ocean grid cells is done by averaging the values in neighbouring oceanic grid cells when necessary. The conservation of the total content of conservative variables (salt, carbon...) is ensured.

Figures

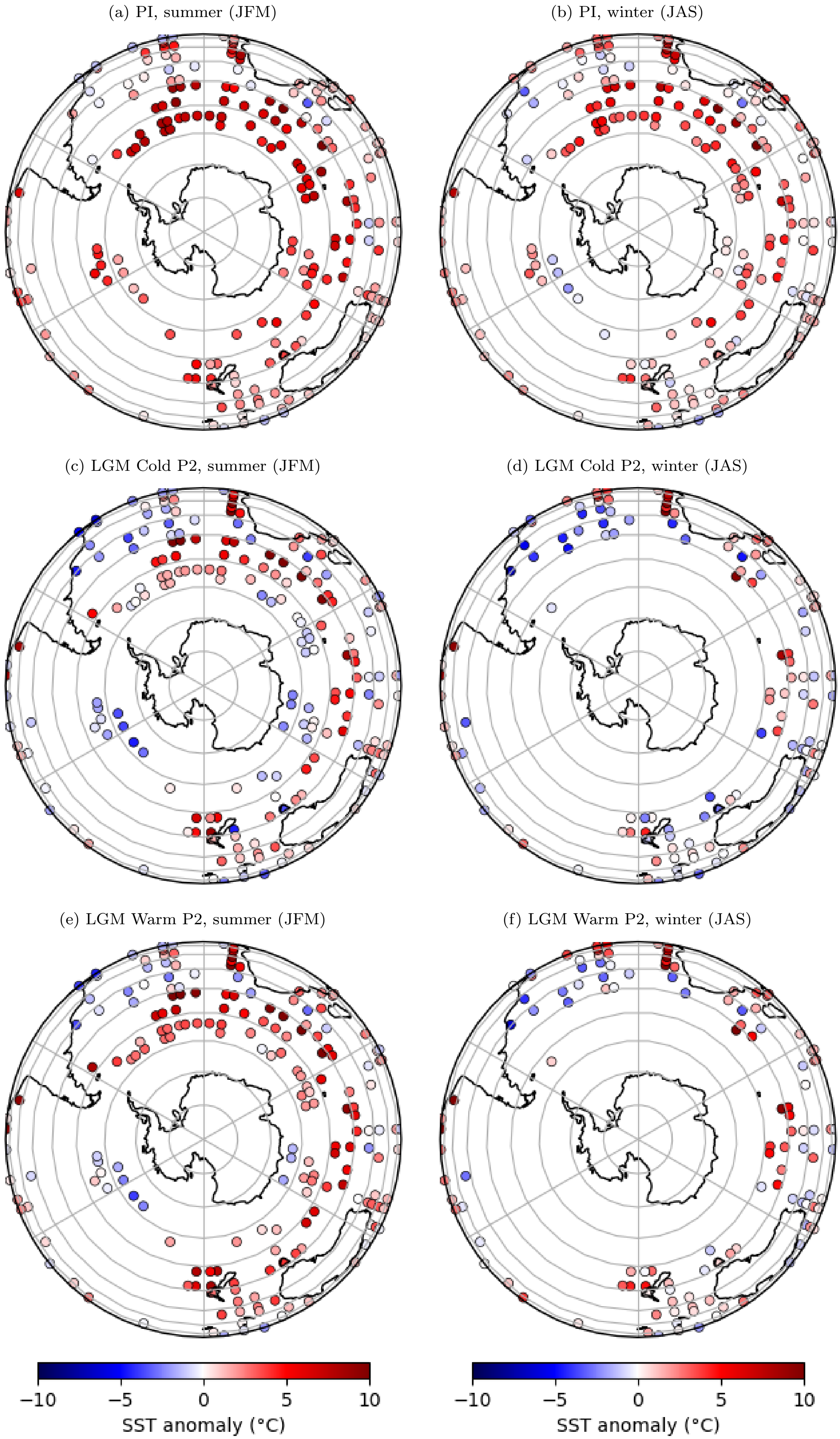
(a) PI, summer (JFM)
(b) PI, winter (JAS)
(c) LGM Cold P2, summer (JFM)
(d) LGM Cold P2, winter (JAS)
(e) LGM Warm P2, summer (JFM)
(f) LGM Warm P2, winter (JAS)
−10
−5
0
5
10
SST anomaly (°C)
−10
−5
0
5
10
SST anomaly (°C)

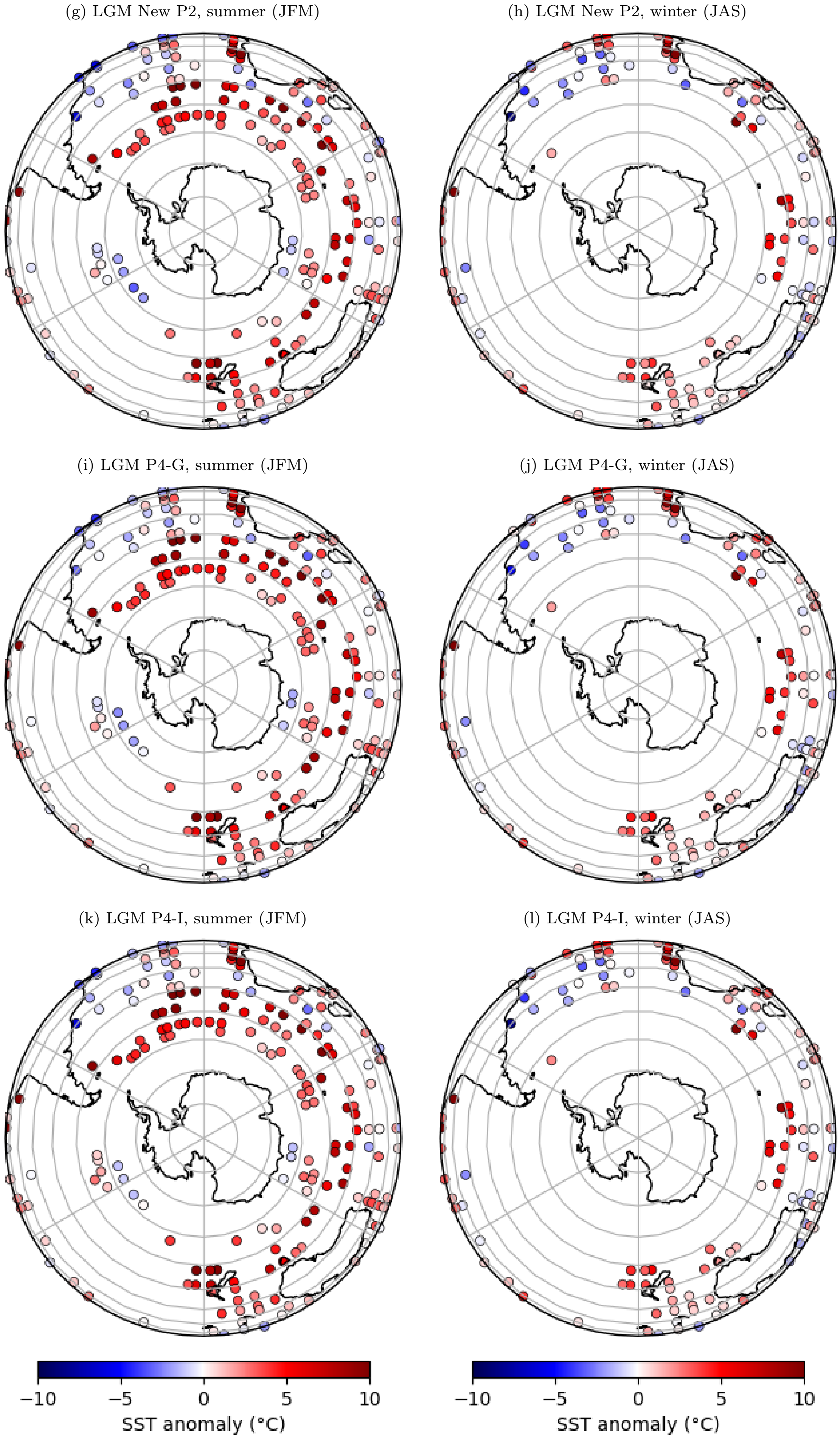
(g) LGM New P2, summer (JFM)
(h) LGM New P2, winter (JAS)
(i) LGM P4-G, summer (JFM)
(j) LGM P4-G, winter (JAS)
(k) LGM P4-I, summer (JFM)
(l) LGM P4-I, winter (JAS)
−10
−5
0
5
10
SST anomaly (°C)
−10
−5
0
5
10
SST anomaly (°C)

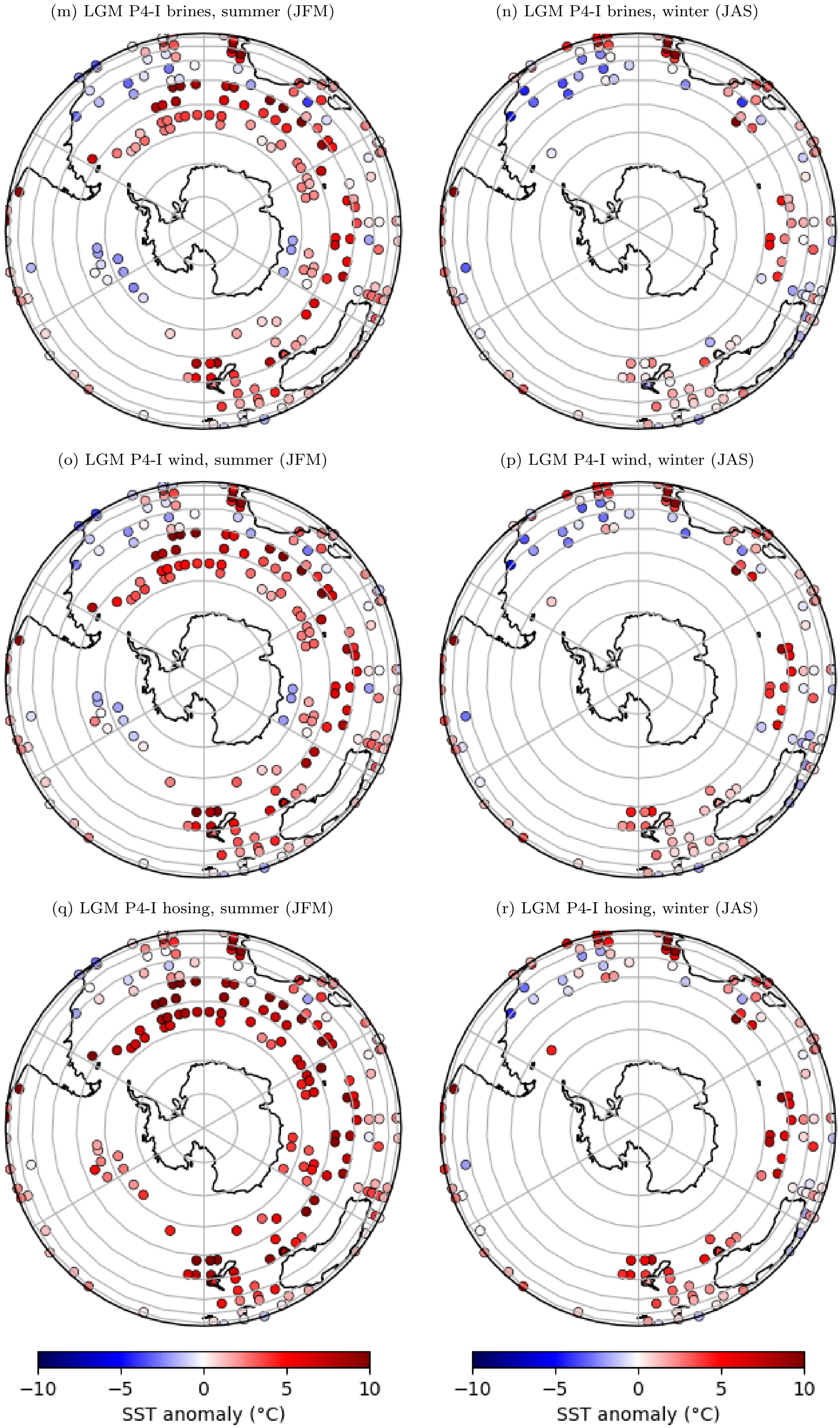

FIGURE S1 – Austral summer (JFM) and winter (JAS) SST anomalies relative to proxy data from the regridded product of MARGO project members [2009].

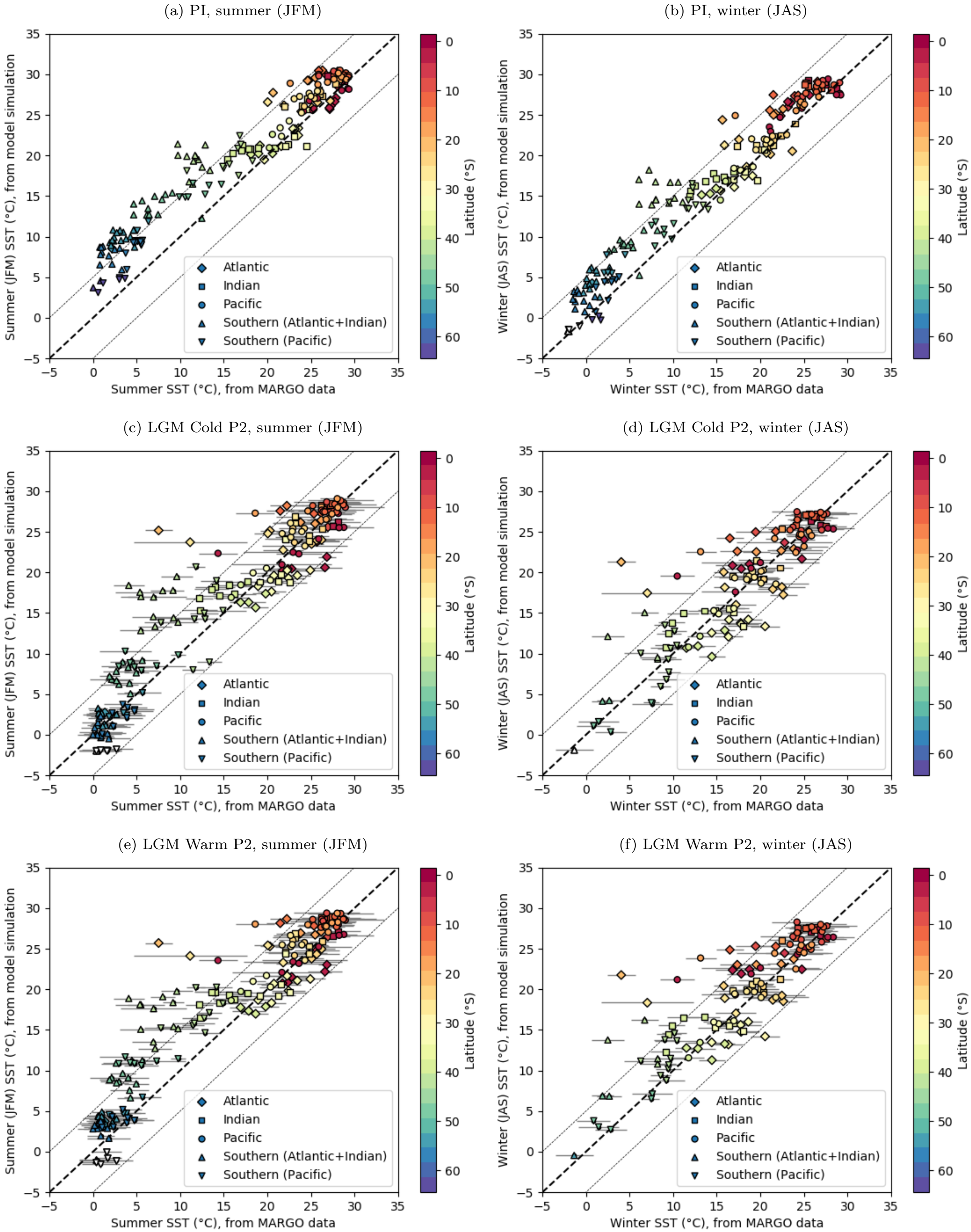
(a) PI, summer (JFM)
(b) PI, winter (JAS)
(c) LGM Cold P2, summer (JFM)
(d) LGM Cold P2, winter (JAS)
(e) LGM Warm P2, summer (JFM)
(f) LGM Warm P2, winter (JAS)
Summer (JFM) SST (°C), from model simulation
Summer SST (°C), from MARGO data
Winter (JAS) SST (°C), from model simulation
Winter SST (°C), from MARGO data
Latitude (°S)
Atlantic
Indian
Pacific
Southern (Atlantic+Indian)
Southern (Pacific)

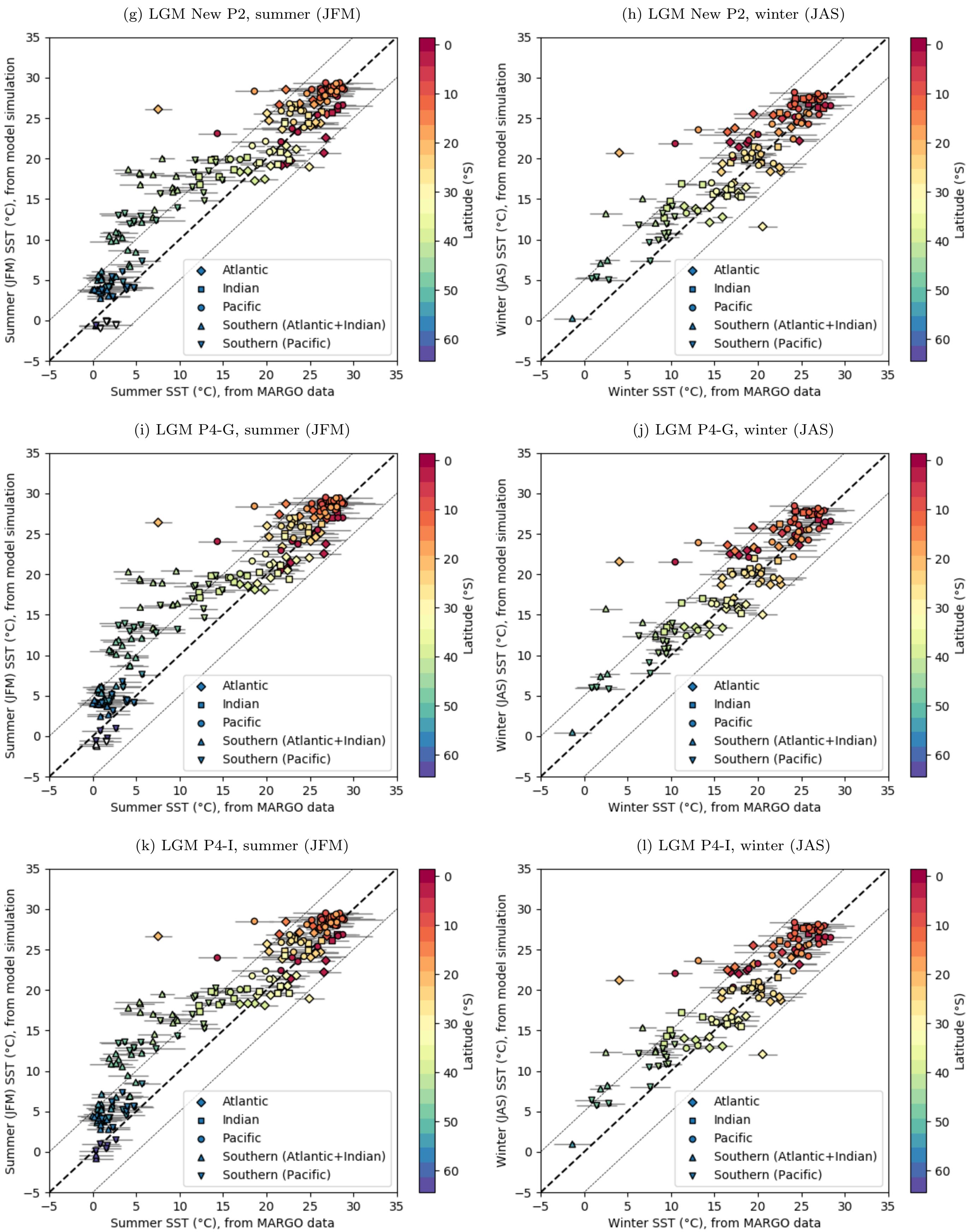
(g) LGM New P2, summer (JFM)
Summer (JFM) SST (°C), from model simulation
Summer SST (°C), from MARGO data
Atlantic
Indian
Pacific
Southern (Atlantic+Indian)
Southern (Pacific)
Latitude (°S)
(h) LGM New P2, winter (JAS)
Winter (JAS) SST (°C), from model simulation
Winter SST (°C), from MARGO data
Atlantic
Indian
Pacific
Southern (Atlantic+Indian)
Southern (Pacific)
Latitude (°S)
(i) LGM P4-G, summer (JFM)
Summer (JFM) SST (°C), from model simulation
Summer SST (°C), from MARGO data
Atlantic
Indian
Pacific
Southern (Atlantic+Indian)
Southern (Pacific)
Latitude (°S)
(j) LGM P4-G, winter (JAS)
Winter (JAS) SST (°C), from model simulation
Winter SST (°C), from MARGO data
Atlantic
Indian
Pacific
Southern (Atlantic+Indian)
Southern (Pacific)
Latitude (°S)
(k) LGM P4-I, summer (JFM)
Summer (JFM) SST (°C), from model simulation
Summer SST (°C), from MARGO data
Atlantic
Indian
Pacific
Southern (Atlantic+Indian)
Southern (Pacific)
Latitude (°S)
(l) LGM P4-I, winter (JAS)
Winter (JAS) SST (°C), from model simulation
Winter SST (°C), from MARGO data
Atlantic
Indian
Pacific
Southern (Atlantic+Indian)
Southern (Pacific)
Latitude (°S)

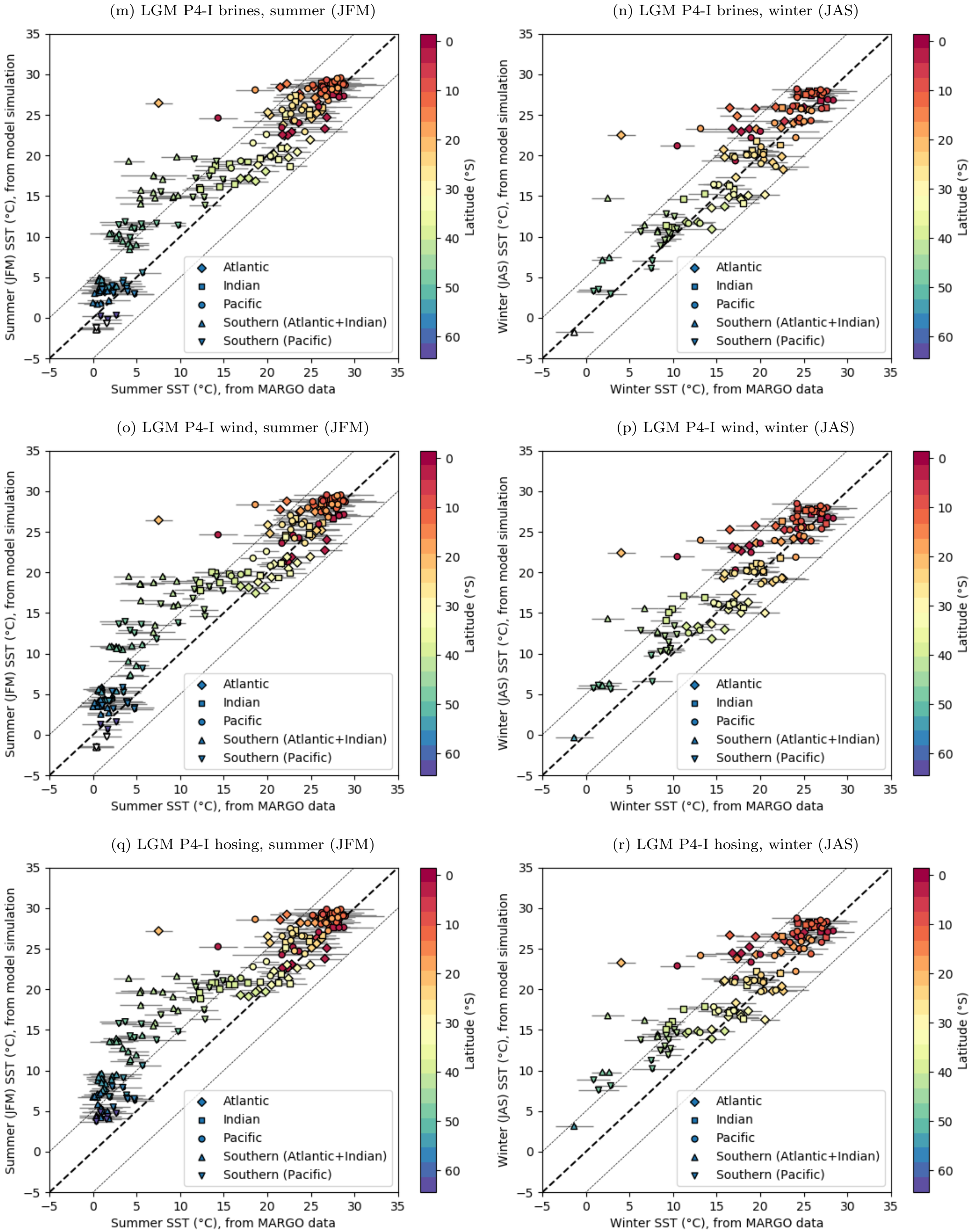

FIGURE S2 – Austral summer (JFM) and winter (JAS) sea-surface temperatures of the Southern Hemisphere in a model versus data diagram, for all simulations. The simulated SSTs are plotted against the SST data from the regridded product (MARGO project members [2009]) thanks to the aggregation of the coordinates on the nearest ocean grid cell. The 1 : 1 line features a perfect model-data agreement. The marker style indicates the ocean basin of each core. The marker color shows the latitude of the core, except it is white where the model simulates sea ice in the Southern Ocean. The uncertainties associated with the SST data are plotted by the grey horizontal bars.

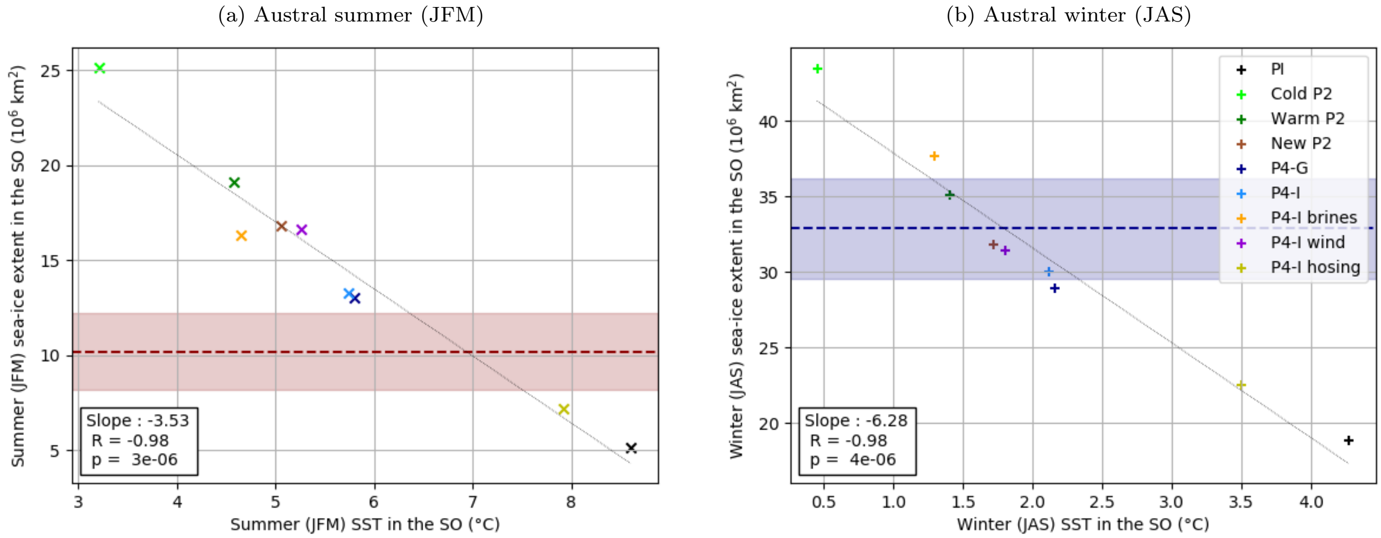

FIGURE S3 – Relationship between the mean SST (averaged up to 36°S) and the sea-ice extent in the Southern Ocean. The LGM sea-ice extent estimated using the proxy data compilation is represented by the red (summer) and the blue (winter) bars.

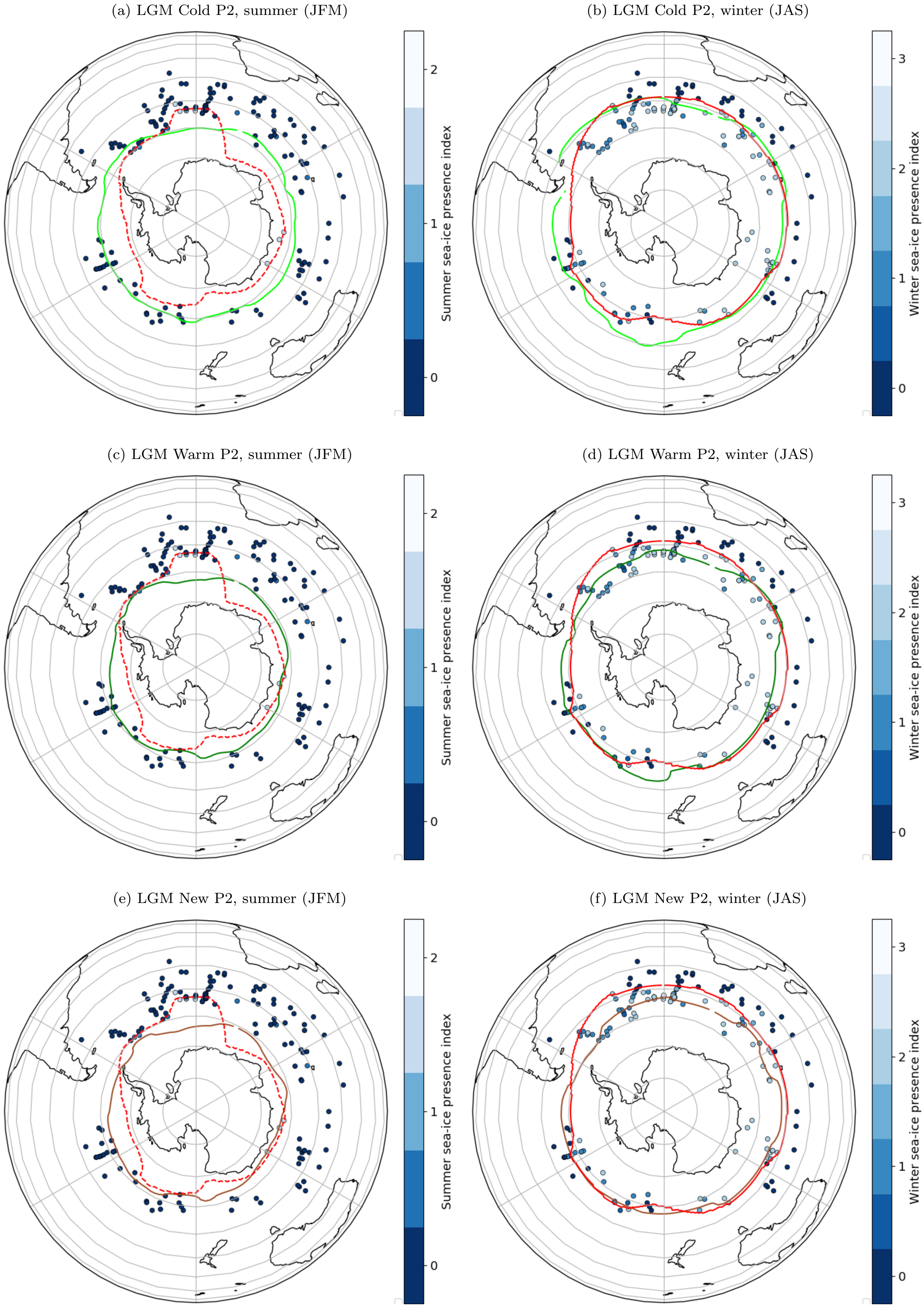

(a) LGM Cold P2, summer (JFM)
Summer sea-ice presence index
0
1
2
(b) LGM Cold P2, winter (JAS)
Winter sea-ice presence index
0
1
2
3
(c) LGM Warm P2, summer (JFM)
Summer sea-ice presence index
0
1
2
(d) LGM Warm P2, winter (JAS)
Winter sea-ice presence index
0
1
2
3
(e) LGM New P2, summer (JFM)
Summer sea-ice presence index
0
1
2
(f) LGM New P2, winter (JAS)
Winter sea-ice presence index
0
1
2
3

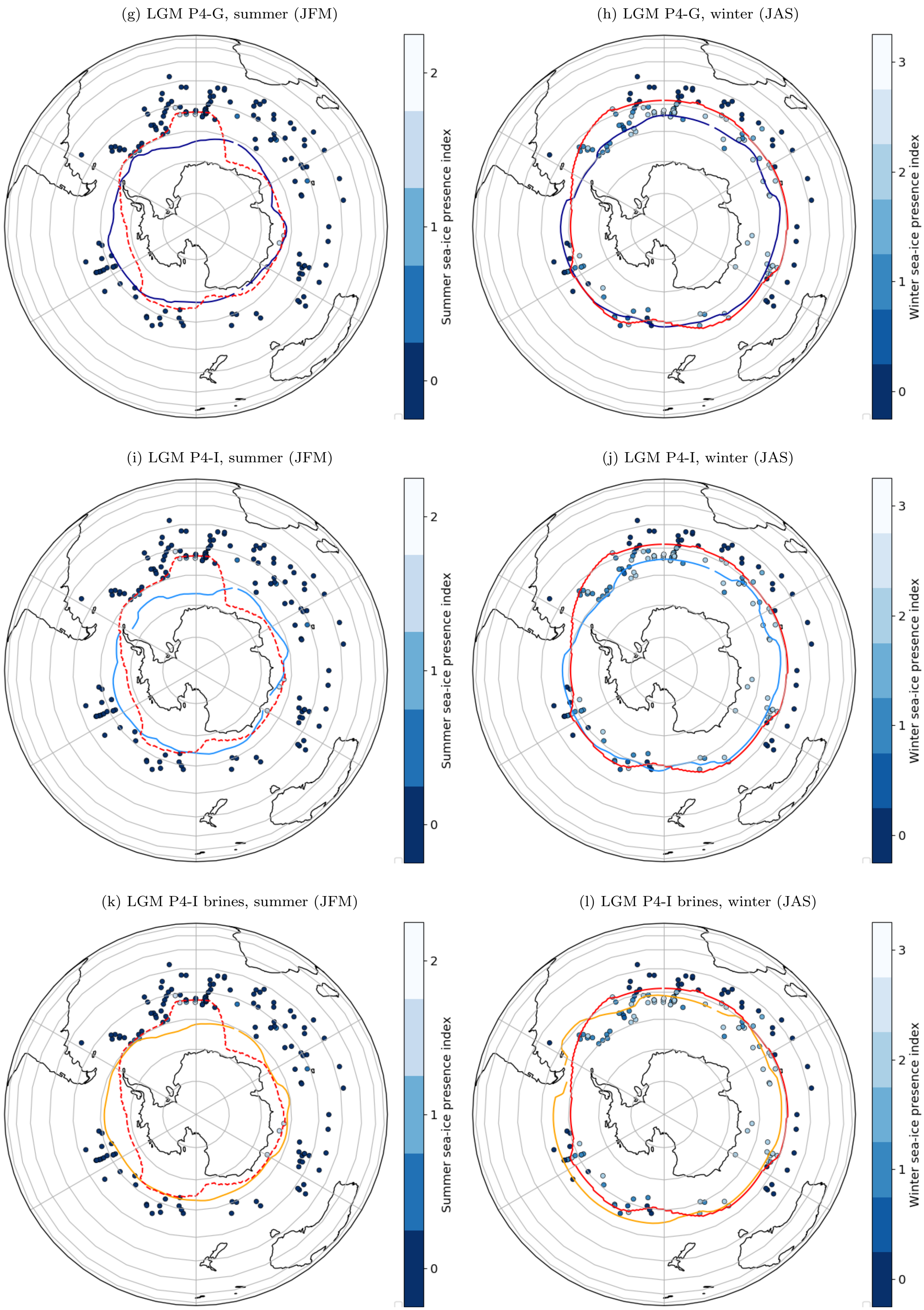

(g) LGM P4-G, summer (JFM)
(h) LGM P4-G, winter (JAS)
(i) LGM P4-I, summer (JFM)
(j) LGM P4-I, winter (JAS)
(k) LGM P4-I brines, summer (JFM)
(l) LGM P4-I brines, winter (JAS)
Summer sea-ice presence index
Winter sea-ice presence index
0
1
2
3

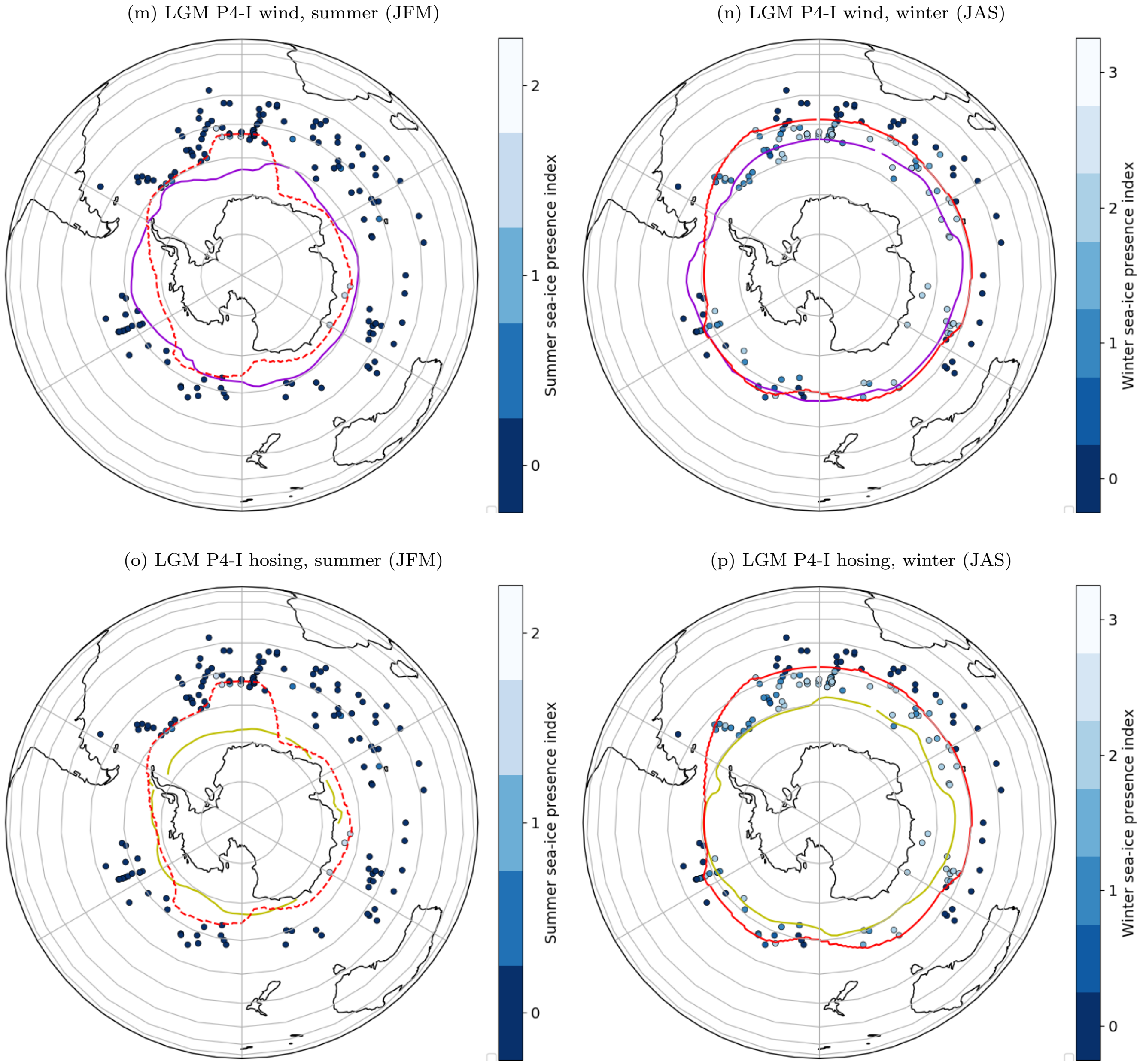

Figure S4 – Austral summer (JFM) and winter (JAS) sea-ice edges (at 15% of sea-ice concentration) in the Southern Ocean. The sea-ice presence suggested by marine cores data is represented as an arbitrary index on a blue (no proxy indicate sea ice) to white (several proxies agree on the presence of sea ice) scale. The red lines mark the likely delimitation of the sea-ice presence according to the proxy data (compilation of data from Gersonde et al. [2005], Allen et al. [2011], Ferry et al. [2015], Benz et al. [2016], Xiao et al. [2016], Nair et al. [2019], and Ghadi et al. [2020]).

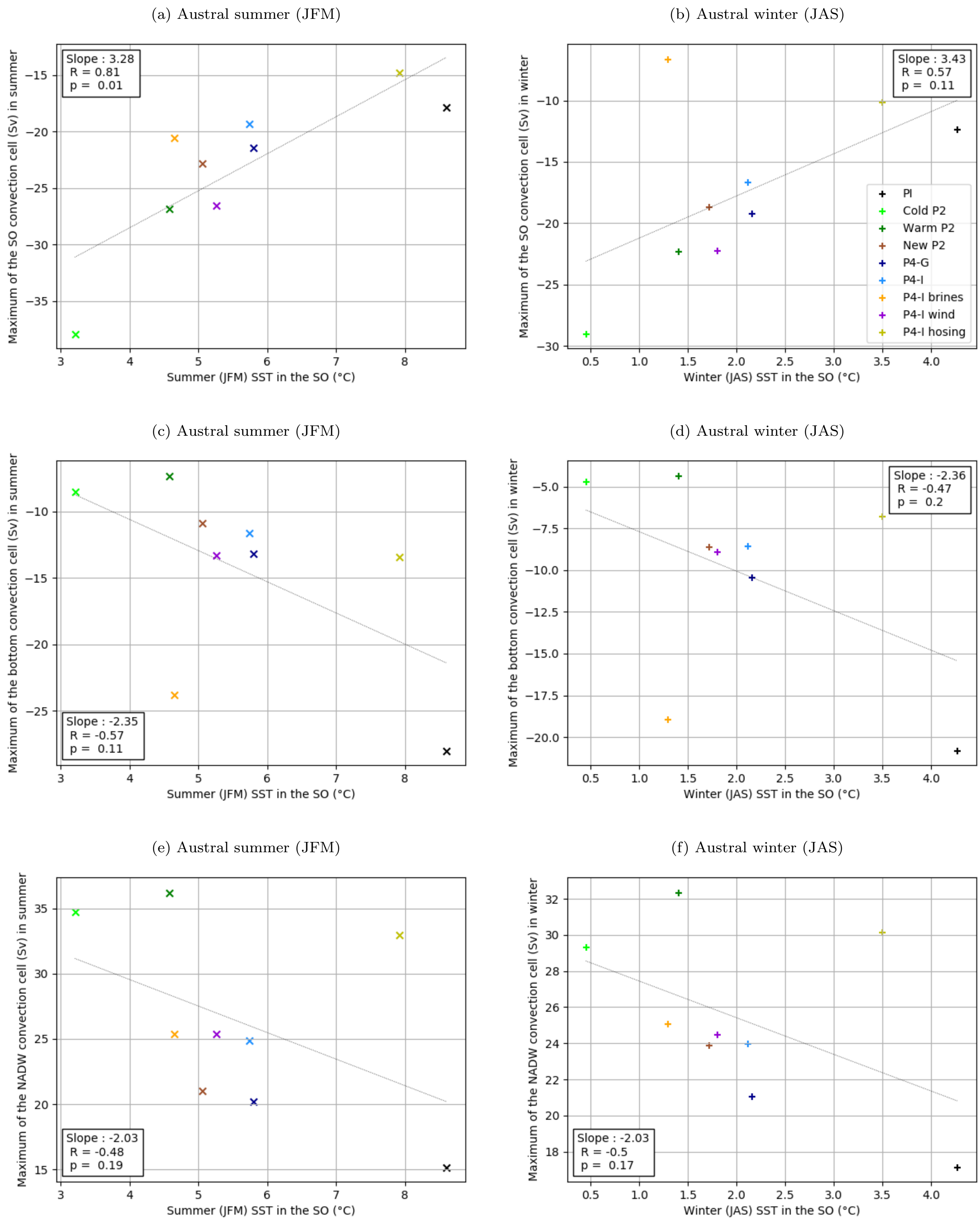

FIGURE S5 – Relationships between the mean SST in the Southern Ocean (averaged up to 36°S) and the Southern Ocean (a, b), bottom (c, d) or NADW (e, f) convection cell maximum for all simulations.